Al-Nahrain Journal for Engineering Sciences **NJES** 27(1)109-117, 2024
http://doi.org/10.29194/NJES.27010109

Characterization and Fabrication of Ankle Foot Orthoses using Composite with Titanium Nanoparticles

N.J. Khalaf [1*], Sabrine Ben Amor[2], Borhen Louhichi[3]

Authors affiliations:
1*) Mechanical Laboratory of Sousse, Higher Institute of Applied Science and Technology of Sousse, University of Sousse, Sousse 4000, Tunisia.
najla.jasim1@gmail.com

2) Mechanical Laboratory of Sousse, Higher Institute of Applied Science and Technology of Sousse, University of Sousse, Sousse 4000, Tunisia.
sabrinebenamor94@gmail.com.
3) Department of Mechanical Engineering, College of Engineering, Imam Mohammad Ibn Saud Islamic University (IMSIU), Riyadh 11432, Saudi Arabia.
blouhichi@imamu.edu.sa

Paper History:

Received: 2nd March 2024

Revised: 9th May 2024

Accepted: 15th May 2024

Abstract

Orthoses and prostheses were Chosen and laminated based on their high Yield, ultimate stresses, bending stresses, and fatigue limit. Response Surface Methodology (RSM) was utilized to find the best values for two parameters reinforcement perlon fiber and percent of Titanium Nanoparticle coupled with the matrix resin during optimization. The response surface methodology combined the expertise of mathematicians and statisticians to construct and analyze experimental models. Using this method, we identified 13 different lamination samples comprising a wide range of perlon number and Ti nano Wt% in their Perlon layer composition. All lamination materials defined by RSM methods and produced by a vacuum system were subjected to a battery of tests, with fatigue tests performed on the ideal laminating material in contrast to laminations created in the first study (Tensile test, Bending test, and Fatigue tests according to the ASTM D638 and D790 respectively). In comparison to the other 12 laminations tested using Design Expert version 10.0.2, the lamination with ten perlon layers and 0.75 percent Ti nano proved to be the strongest overall in terms of Yield, ultimate, and bending loads. This study used composite materials and titanium nanoparticles to characterize and fabricate ankle foot orthoses. Strength in bending should amount to about 70 MPa, around 85 MPa in tensile tension. Two empirical quadratic equations for the models of peak bending strength and maximum tensile stress with 95% confidence were created using the response surface approach and analysis of variance within the design of experiments software.

Keywords: Components Life Extension (Recycle), Cracked Shaft, Plastic Deformation, Laser Shock-Peening, Compressive Residual Stress, Mechanical Properties, Dislocation Strengthening Mechanism.

1. Introduction

Orthoses are devices that improve a patient's quality of life by alleviating pain, correcting a deformity, strengthening a weakened muscle, increasing mobility, or regulating spastic muscle activity [1]. Other considerations like prices and feasibility are crucial in signaling a lightweight, durable, and individualized orthosis [2]. Orthoses that fulfill these requirements may soon be produced using cutting-edge technology. Carbon nanotubes (CNTs) have piqued the interest of scientists, communities, and enterprises due to their exceptional qualities, such as high electrical and thermal conductivity, a long lifespan, and a solid modulus. Because of their large specific surface area, CNTs are an effective means of transferring stress. However, it can generate substantial and alluring forces between CNTs, which can cause unneeded strain and lead to excessive stress and eventual collapse. Due to their larger diameter and more walls made of graphene, multi-walled carbon nanotubes (MWCNTs) are less dense than single-walled carbon nanotubes (SWNTs) [3]. Numerous researchers have delved into orthotics, and efforts have been made to improve the construction of orthotics by altering the mechanical properties of the materials used to create them. Bedaiwi et al. [4] conducted experimental research into the vibration behavior of below-knee prostheses in 2012. Then, Chiad [5] investigated the low-velocity impact behavior of prosthetic limbs in 2014. In 2017, Al-Shammari et al. [6] used experimental and numerical techniques to examine stress analysis and mechanical properties of knee sockets. Multiple researchers in 2018 looked at various characteristics, including other structures' mechanical qualities and behavior.

Tahir et al. [7] Suggested a new material to manufacture orthoses and orthoses sockets containing an experimental study of the mechanical characteristics of the materials. Then, Abbas et al. [8] looked into the fatigue behavior of a composite-made half foot. JS Chiad, MS al-Din Tahir [9] enhanced the mechanical properties of the composite materials used in prosthesis and orthoses sockets. Jweeg et al.

NJES is an **open access Journal** with **ISSN 2521-9154** and **eISSN 2521-9162**
This work is licensed under a Creative Commons Attribution-NonCommercial 4.0 International License

[10] also used computational approaches to construct optimal prosthetic sockets. Syme's prosthesis fatigue behavior was calculated using an experimental technique by Abdulameer et al. [11]. The stress distribution in the knee joints was determined by Yaseen [12] using the photo-elasticity method and compared to numerical results. The impact of carbon reinforcing fiber on foot orthosis mechanical analysis behavior was studied by Takhakh et al. [13]. The gait cycle and mechanical properties of below-knee sockets were also the subjects of an experimental study by Takhakh et al. [14]. They also used numerical methods to predict the socket's mechanical performance. Using experimental and numerical methodologies, Kadhim et al. [15] employed smart transfemoral to fabricate and design prosthetic knee joints. Yousif et al. [16] used experimental methods to determine the foot's mechanical properties and numerical methods to determine its mechanical behavior as they studied the impact of temperature on its mechanical properties and behavior. Lower limb feet were manufactured by Oleiwi et al. [17] using composite polymer blends, which were analyzed for mechanical properties using an experimental approach, and the mechanical behavior of the foot was subsequently calculated using a numerical technique. In addition, Jweeg et al. [18] used a CT scan to investigate the dynamic behavior of the lower leg in 2019. Using a CT scan model, they looked into the dynamic stress and deformation below the knee. Kadhim et al. [19] looked at how using various reinforcing fibers altered sockets' mechanical characteristics and behavior. Abbas et al. [20] looked at fatigue characterizations of prosthetic sockets produced from various laminated composite materials using experimental methods in 2020. Then, Kadhim et al. [21] employed amputees of the knee joint to analyze several types of prosthetic knees using experimental and numerical methods. Kadhim et al. [22] also used experimental and numerical methods to delve into the smart economical prosthetic. Researchers from various disciplines have also studied how nanoparticles modify composites' physical and mechanical characteristics. The impact of nanoparticles on the mechanical characteristics of Bioimplants was studied by Mohammed et al. [23]. The impact of nanoparticle coating on fatigue characterization for steel materials was studied by Al-Shammari et al. [24], who used numerical and experimental methods. Al-Waily [25] used analytical and numerical methods to investigate how the presence of nanoparticles altered the thermal buckling behavior of composite materials. Ankle-foot orthoses (AFOs) must be as lightweight and patient-friendly as feasible because of their design's wide variety of uses. The material must be both inexpensive and have excellent mechanical characteristics. Ahmed et al., 2020 (26), and Rajan et al., 2021 (27)). According to the findings of these investigations, nanoparticles have the potential to greatly improve the mechanical characteristics and performance of AFOs. Using composite materials, Khandagale and Pise 2022(28) sought to increase the strength and longevity of an ankle-foot orthosis (AFO). The complicated anatomy of the leg and ankle led the researchers to employ 3D modeling and printing. Newly built equipment for testing the stiffness of ankle-foot orthoses (AFOs) in frictionless conditions was reviewed by Rogati et al. in 2022 [29]. Using 3D printing, Shahar et al. 2022 [30] investigated the potential of a natural composite filament produced from kenaf and polylactic acid (PLA) for creating ankle-foot orthoses (AFOs). Below-knee socket prosthetic devices are often fabricated from composite laminated materials with varying reinforcing fibers; Jweeg et al. 2021 [31] studied the effect of varying Nanomaterial types and weight fractions on stress and deformation in these materials. Zakaulla et al. 2022 [32] investigated the effects of varying amounts of graphene and titanium powder on high-performance PEEK hybrid composites' production and mechanical properties. Al-Maliky, F.T., Chiad, J.S.[022[33], study and measured the kinematic data of patient suffering from transfemoral amputation. Tahir, M.S.A,2022[34] study and analysis the Kinematic parameters for passive multi-axes ankle joint during daily activity for the patient suffering from SYMS amputation.

These composites have several potential uses. The literature review reveals much research into nanomaterials and their application in enhanced mechanical characteristics, as well as the modeling of ankle-foot orthoses (new design and optimization of AFO).

2. Materials and Methods:

2.1 Laminations of Ankle-Foot Orthoses:

Orthoses and prostheses, as well as specimens for mechanical testing, are primarily made from the following materials:

1. The stockinet is made of Perlon (Ottobock Health Care 623T3). Nylon 6, also known as Perlon, is created through a series of drawing and melting steps. Because of its high energy content, excellent heat resistance, and high density, Fig. 1.a.
2. Glass fiber (ottobock health care 616G13) ,fig .1.b
3. Ti nonparties / Nanopowerds have outer diameter (30 -50) nm, Fig.1.c
4. Polyurethane lamination resin (otto bock healthcare 617H19, an 80/20 mixture)is used in laminations. Polyurethane resin is typically formed when a diisocyanate reacts with a polyol. Foams, elastomers, and liquid coatings are all available forms of the material ,Fig.1.d
5. Ottobock medical 99B71 polyvinylalcohol (PVA) bag. PVA placement to separate composite material from mold and sandwich matrix blend between two PVAs, Fig. 1.e
6. The powder used to harden the composite material is (otto bock health care 617P37), Fig.1.i

Figure (1): Materials used to manufacture AFO laminations (a) Perlon stockinet white, (b)glass fiber (c) Ti nanoparticles, (d) polyurethane resin, (e)Polyvinylalcohol PVA bag, (i) hardening powder.

The main types of equipment used in manufacturing ankle-foot orthoses laminations are shown in Fig. 4-2 and describe below:

1- A gypsum mold has the dimensions of a parallelogram (20*12*24) cm³, Fig. 2. a.
2- The vacuum apparatus consists of a pump, pipes, and a suction cover is shown in Fig 2. b.
3- Ultrasonic mixing device, ultrasonic device type Hielscher and ultrasonic processor UP200Ht were utilized as shown in Fig. 2.c. Ultrasonic device contains ultrasonic generator, probe and setting with 26 KHz and 160 Watt for 60 minutes [35] to make mixing between Ti nanoparteas and polyurethane resin with different weight percentage (0,0.25,0.5,0.75,1) % Wt. loading. The process of the mixing performed according to safety recommendations by Cheap Tubes Company [36].
4- Sensitive scale device with three digits that used to weight Ti nanoparticles and to calculate physical properties of the composite material, Fig. 2-d.

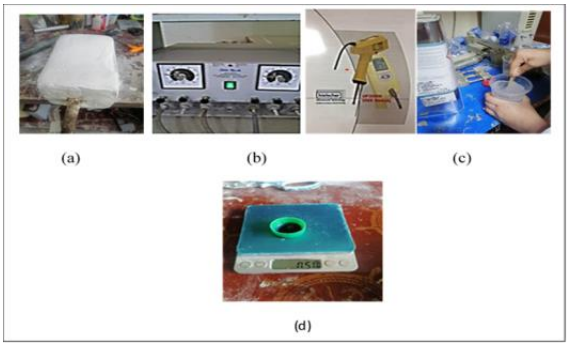

Figure (2): Equipment's used to manufacture AFO laminations, (a) gypsum mold, (b) vacuum device, (c)ultrasonic device, (d)sensitive scale device.

2.2 Ankle Foot Orthoses Laminations with Design Parameters

Mechanical workshops were also utilized for shaping and cutting different types of forms. Ankle foot orthoses (AFO) feature characteristics are laminated using practical knowledge and analytical method limitations to determine experimental input parameters [37]. Therefore, the measured parameters are the number of Ti nanolayers and Perlon layers. Between 0% and 1% of titanium nanoparticles is added to 80:20 lamination resin, while Perlone useed between 4 and 12 layers (Table 1) throughout 13 trials. The DESIGN-EXPERT v10.0.2 software is used to develop the blueprint. The samples were cleaned and AFO orthodontics were made using the vacuum lamination method. Mechanical workshops were also utilized for shaping and cutting different types of forms. Ankle foot orthoses (AFO) feature characteristics are laminated using practical knowledge and analytical method limitations to determine experimental input parameters. Therefore, the measured parameters are the number of Ti nanolayers and Perlon layers. Between 0% and 1% of nano titanium is added to 80:20 lamination resin, while Perlone uses between 4 and 12 layers (Table 1) throughout 13 trials. The DESIGN-EXPERT v10.0.2 software is used to develop the blueprint. The samples were cleaned and AFO orthodontics were made using the vacuum lamination method.

Table (1): Suggested experiments (runs) by RSM.

Runs No.	Exp. No	glass fiber	Ti NPs (%)	Perlon (layers)
1	3	1	0.25	6
2	4	1	0.75	6
3	8	1	0.25	10
4	7	1	0.75	10
5	6	1	0	8
6	5	1	1	8
7	1	1	0.5	4
8	9	1	0.5	12
9	2	1	0.5	8
10	10	1	0.5	8
11	11	1	0.5	8
12	12	1	0.5	8
13	13	1	0.5	8

2.3 Mechanical Test

a. Tensile test:

Tensile test is widely used in materials research for determining mechanical properties, including yield stress, ultimate stress, Young's modulus, material density, and so on [38,39]. ASTM International (previously the American Society for Testing and Materials) Standard D638 [40] was used to shape and size all specimens. As can be seen in Fig.3, two different specimen shapes (I and IV) were used and cut using a laser computer numerical control system (CNC) by ASTM [61-66]. All samples were subjected to strain testing at a 2 mm/min rate.

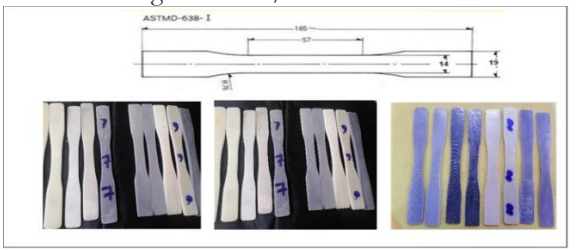

Figure (3): Specimens of the tensile test.

b. Bending test:

Three samples from each lamination (run) were put through tests with the Standardised Measuring Instrument (Testomertic) for three-point bending flexures. About Fig. 4, CNC samples were lasered by ASTM D790-03-9, and three pieces at 5 mm/min crosshead speed and 25 kN capacity were examined to determine the best substrates for each lamination.

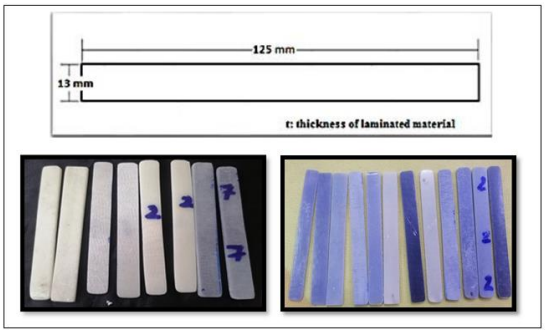

Figure (4): Dimensions and specimens of the bending test.

c. Case study and patient tests

The kinetics and kinematics data were collected for the patient with age, height, and weight 15 years, 166cm, and 45kg respectively. As shown in Fig.5, the patient had an ankle-foot orthosis (AFO) to prevent plantarflexion and dorsiflexion of the flat foot. 5. Planovalgus and anteversion, flat foot with foot distortion, are congenital conditions that affected the patient in this case study.

Figure (5): Case study of the patient flat foot.

d. Gait cycle and ground reaction force (GRF) test:

This work was carried out using force plate (Tekscan Walkway Pressure Measurement Systems) devices. T-Scan transmits data from the device to a computer to be analyzed. This data includes measurements of the unit's GRF and foot scanning over a force plate, data on the gait cycle's location and swing phase, and the alignment and discrepancy between the abnormal and normal legs. Data from the left (defects leg) and right (normal leg) legs were compared in two settings (with and without orthosis of the knee foot; see Fig. 6. As can be seen in Fig. 7, the patient was given two trials of walking on a force plate without the aid of crutches. Also, the PWD details were listed in table 2.

Figure (6): The force plate (Walkway) device.

(a) (b)

Figure (7): patient with force plate device (a) with wearing AFO, (b)without wearing AFO.

Table (2): PWD details

Item	Gender	Age	Weight(kg)	Hight(cm)	Type of Orthoses
1	Male	15	45	166	AFO

e. Measuring of interface pressure.

Due to the AFO's ability to correct abnormalities, the patient's leg will alternate between resting on the AFO and the knee and touch area. The device's strain measures this charge. Mat-Scan examined three different regions of the AFO (inside, outside, and behind; see Fig. (8) for details). These are the zones where the efficacy of the delivery is evaluated. The gathered touch pressure is employed as boundary conditions in the numerical analysis.

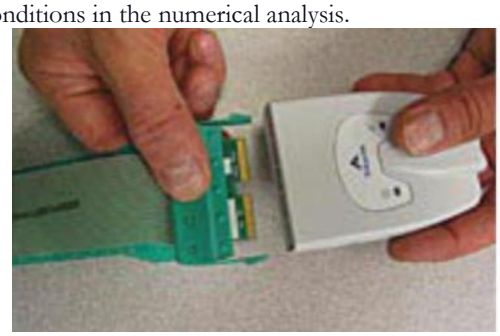

Figure (8): The Mat-Scan sensor.

Figure (9): Patient walking with Mat-Scan sensor and AFO (internal lateral side, external lateral side and rear side)

3. Results and Discussion

3.1 Mechanical properties

The results of the patented mechanical testing, tensile testing, three points of flexure test, bending test, and fatigue test on all laminating materials are shown in Table (3). Later, the fatigue test results and the material's yield stress, strains, ultimate stress, Young's modulus, elongation, and other properties to were used to simulate the ankle-foot orthoses and analyze the stress, deformation, and safety factor using ANSYS 22.1 Software. The Testometrec tensile test apparatus was used to conduct tests on three samples for each run, with room temperature as the testing environment. From the strain-stress curve, the tensile test properties of all lamination material (runs) are tabulated in Table.3. Two input parameters (weight percentage of Ti nanoparticles and no. of Perlon layers) were found to affect the mechanical stresses and modulus of elasticity. As the percentage of Ti nanoparticles in the matrix (lamination resin) was raised, it was found that the yield stress and other parameters also rose. Because of the exceptional stiffness and strength, high flexibility, diameter-dependent specific surface area, and high aspect ratio of Ti nano, this mixture alters the properties of lamination resin. Additionally, the mechanical properties of the composite materials improved as the number of layers of reinforcement material (perlon fiber) increased.

Table (3): Mechanical properties of all runs of lamination materials

Run No.	Exp. No.	Fiber glass	Ti NPs (%)	Perlon (No. of layer)	Yield stress MPa	E GPa	Max. tensile stress (MPa)
1	3	1	**0.25**	**6**	**82**	**1**	87
2	4	1	**0.75**	**6**	**70**	**2**	76
3	8	1	**0.25**	**10**	**69**	**2**	75
4	7	1	**0.75**	**10**	**74.4**	**2**	88
5	6	1	**0**	**8**	**54**	**1**	60
6	5	1	**1**	**8**	**75**	**1**	81
7	1	1	**0.5**	**4**	**70**	**1**	76
8	9	1	**0.5**	**12**	**70**	**1**	70
9	2	1	**0.5**	**8**	**54**	**1**	86
10	10	1	**0.5**	**8**	**57**	**1**	90
11	11	1	**0.5**	**8**	**65**	**1**	84
12	12	1	**0.5**	**8**	**68**	**1**	88
13	13	1	**0.5**	**8**	**52**	**1**	90

The least-squares method was used to calculate the models of the response surface for each response based on the average responses determined for the highest tensile stress. In terms of mechanical variables, the ultimate tensile stress equation is:

Maximum tensile stress = 78.01437- 49.41379* Ti NPs +5.22989* Perlon + 17.00000* Ti NPs * Perlon-68.58621* Ti NPs^2 - 0.91541*Perlon^2 ……(1)

A simplified quadratic model in coded terms was analyzed by backward eliminating unimportant factors to predict maximum tensile stress. There is a 95% chance that the model is meaningful. The p-values for the numbers of titanium nanoparticles (A), perlon layers (B), their interaction (AB), and their squares are all less than 0.05, making them valuable.

A decent model will fail the goodness-of-fit test. This model shows that the maximum tensile stress is most affected by the components (A) and (C), while the term (B) only somewhat affects the tensile strength. Figure 10 shows a typical probability plot for the top tensile stress data, indicating that the residuals, which lie along a straight line and represent errors, follow a normal distribution. Figure (11), which displays the residuals vs the expected responses for the maximum tensile stress data, also reveals the absence of any glaring patterns or atypical structures, suggesting the accuracy of the models.

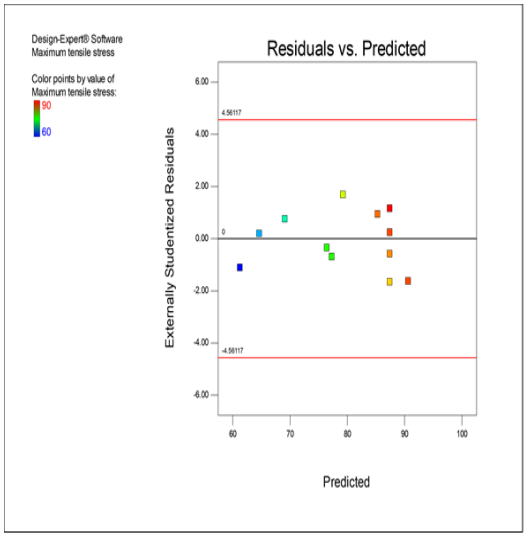

Figure (10): Normal probability plot of normal probability plot of residuals of the maximum tensile stress

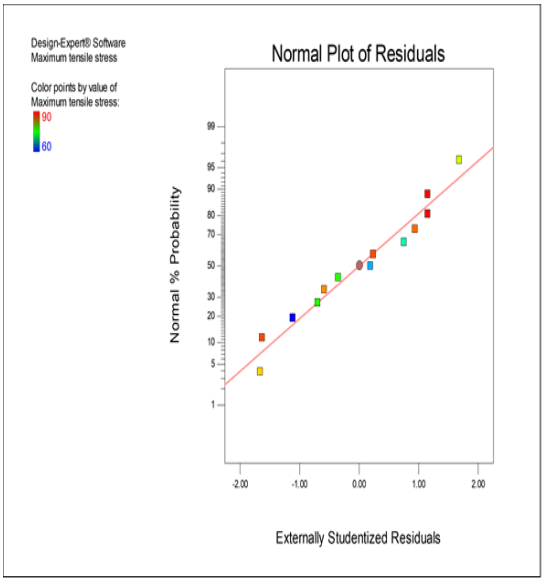

Figure (11): Residuals versus predicted of the maximum tensile stress

Maximum tensile stress versus titanium nanoparticle concentration and sample size (surface plot, Figure 12) validates the results. The ultimate tensile stress value increases when the concentration of titanium nanoparticles and the number of perlon fibers rise. That is to say, the same explanation as

before applies here. Maximum tensile stress is affected more by the percentage of titanium nanoparticles than by the number of people, with lower levels (0.25% titanium nanoparticles and 6 no. of people) reducing the value of ultimate tensile stress.

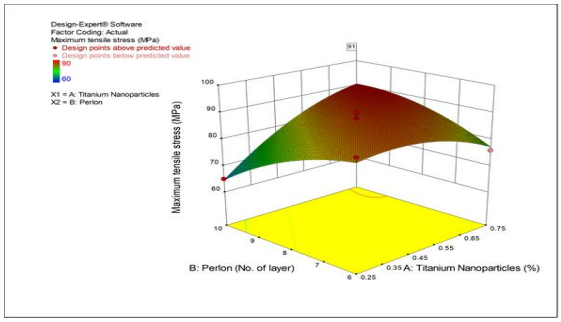

Figure (12): 3D surface plot of tensile at peak in terms of the Titanium nanoparticles and no. of Perlon layers

3.2 Results of the three-point flexural test:

The three-point flexural test was conducted with the help of the Testometric instrument. The average value of three samples was used for each lamination material (run) with various Ti nanoparticles and many perlon layers. The load-deflection curve for each test run is shown in Table 4, and the results (Peak Bending Strength, Yield Bending Strength, and Bending Modulus) are tabulated there. There is a clear correlation between the percentage of Ti nanoparticles, the number of perlon layers, and the bending stress magnitudes.

Table (4): The results of Bending Strength at Peak, Bending Strength at Yield, and Bending Modulus.

Run No.	Exp No.	F.G. Layer	Ti NPs (%)	Perlon (No. of layer)	Bend. Str. at peak (MPa)	Bend. Stre. Yield (MPa)	Bend. E (MPa)
1	3	1	0.25	6	84.103	16.667	2941.7
2	4	1	0.75	6	31.731	6.058	761.991
3	8	1	0.25	10	62.740	12.692	1659.998
4	7	1	0.75	10	94.200	20.262	2459.587
5	6	1	0	8	69.014	13.125	1703.68
6	5	1	1	8	62.308	12.332	1534.907
7	1	1	0.5	4	37.436	7.692	772.323
8	9	1	0.5	12	75.865	15.216	1843.297
9	2	1	0.5	8	69.516	14.131	1872.984
10	10	1	0.5	8	69.516	14.131	1872.984
11	11	1	0.5	8	69.516	14.131	1872.984
12	12	1	0.5	8	69.516	14.131	1872.984
13	13	1	0.5	8	69.516	14.131	1872.984

The least-squares method was used to generate the response surface models for each response based on the average responses determined for peak bending strength. A simplified quadratic model in coded terms was analyzed by backward eliminating unimportant coefficients to predict bending potency at height. The software's analysis of variance (ANOVA) for the remaining terms is displayed in Table 5.3. There is a 95% chance that the model is meaningful. It is noted that the squares of Titanium nanoparticles (A2) and perlon (B2), as well as their interaction (AB), are essential concepts. A decent model will fail the goodness-of-fit test. Since their P-values are smaller than 0.05, this model shows that these factors significantly affect the peak bending strength.

The final equation for peak bending strength in terms of physical variables is:

Bending Strength at Peak=178.66592 - 331.49233* TiNPs -10.96350*Perlon + 42.64900* TiNPs* Perlon -19.31900* $TiNPs^2$- 0.33377* $Perlon^2$ ……(2)

The residuals, which generally lie on a straight line signifying errors, are frequently distributed, as shown in the conventional probability plot (figure 13) for bending strength data.

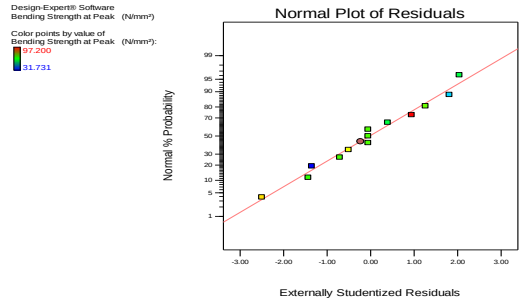

Figure (13): Normal probability plot of residuals of the bending strength at peak

Figure (14) examines a three-dimensional graph (surface plot) of peak bending as a function of Ti percentage and perlon count, corroborating the previous findings. The bending strength increased with both the Ti percentage and the number of perlon layers, reaching a maximum of 10 perlon layers and 0.75 percent Ti. The same justification as before is given for this. This improvement can be attributed to the enhanced interface and dispersion of titanium nanoparticles throughout the polyurethane matrix.

However, if the titanium nanoparticles are not dispersed, and there is poor adhesion between them and the matrix material, the flexure properties will suffer. Similarly, if the titanium nanoparticle weight percentage is too high, the resin will become too thick to process bubbles and impurities. The maximum bending stress value also grows as the number of perlon layers rises. As reinforcement fiber content was raised, bending stress increased because of the better composite material characteristics and the more cohesive interface between the additives (Ti nanoparticles and perlon layers). When the number of perlon layers was at its most minor (6 layers), the effect of perlon was at its weakest; at its strongest (0.75% Ti), the bending stress reached about (31.4 MPa). However, titanium nanoparticles' minimum weight percentage of Ti% was 0.25 percent, and the maximum value of the number of perlon layers was 10 percent, yielding a peak bending strength of around 60 megapascals (MPa)

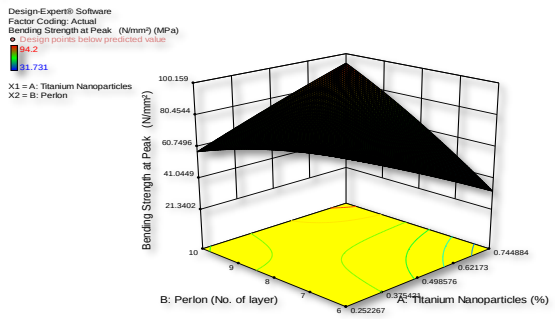

Figure (14): 3D surface plot of bending at peak in terms of the Titanium nanoparticles and no. of Perlon layers.

3.3 Results of Numerical Optimization.

In light of the numerical optimization, the tests were planned to find the best possible parameter settings that meet the requirements. Reactions, yield stress, global stress, and mass have all been measured using the technique. These numbers depend on the number of layers of perlon and a Ti nano. In this endeavor, there is no priority hierarchy among the variables (render anxiety, final stress, maximum bending stress, and unit weight/area). The primary objective of this optimization was to simultaneously evaluate the best possible solution for all attributes of the individual components. As seen in Table (4), only one vehicle satisfies the requirements set out for the optimal yield value, maximum bending stress, and weight.

Table (4): Comparison between the experimental and predicted results for bending at peak and maximum tensile stress

Ti NPs %	No. of Perlon layer	Exp. Bend. at Break (MPa)	Pred. Bend. at Break (MPa)	Exp. Max. tensile stress (MPa)	Pred. Max. tensile stress (MPa)	Error (%)
0.75	10	94.200	94.151	---	---	0.05
0.75	10	---	---	88	90.632	2.90

3.4 Gait cycle properties and GRF Test

The force plate platform was used to conduct two tests on patient processes. The patient walked without the AFO in the first case and with the AFO in the second. Without an AFO, it was discovered that there is a (0.06) second discrepancy between the right foot and the left foot during gait, whereas, with an AFO, this gap is reduced to (0.03) seconds. Manufactured AFO reduces the differences in stance and swing time from (0.04) and (0.09) seconds without AFO to (0.03) and (0.02) seconds with AFO. It also reduces the differences in step length, velocity, and width. As a result, the orthosis helped realign the foot and restore normal function to the affected foot muscles. The critical differences between cases with and without AFO are mirrored in Table 6. As a result of the orthosis correction afforded by the AFO, there is now less noticeable variance in step length, step size, and step width. Table (6) compares and contrasts the two scenarios where AFOs are not worn.

Table (6): Symmetry of gait cycle.

Step-Stride	Patient	
	With AFO	Without AFO
Step Time (sec)	0.08	0.14
Step Length (cm)	7.5	16.5
Step Velocity (cm/sec)	1.6	4.7
Step Length /Leg Length (ratio)	0.16	0.34
Step width (cm)	0.02	0.04
Maximum Force (%BW)	2.5	-10.8
Maximum Force (N)	14.66	-63.37
Impulse (%BW*sec)	1.3	-4.7
Impulse (N*sec)	7.43	-27.51
Maximum Peak Pressure(kPa)	-12	-27
Gait Cycle Time	0.03	0.06
Stance Time	0.03	0.04
Swing Time	0.02	0.09

4. Conclusions

The mechanical qualities have been rated based on the number of Perlon layers and the proportion of titanium nanoparticles. The most important takeaway is that the mechanical attributes can be enhanced by increasing the number of Perlon layers and incorporating the recommended Ti nanoparticle.

1- With the best values for Yield, ultimate, and bending stress, as shown below, the best lamination is (0.75% Wt. Ti nano and 10 Perlon layers), as proved by laboratory test and RSM technique results; -

a- Peak bending strength increases with the percentage of titanium nanoparticles and the number of perlon layers, although the two inputs rise in inverse proportion. The bending power at height is more sensitive to the number of Perlon layers than the fraction of titanium nanoparticles. The result is a bending strength of around 70 MPa or about 0.375% titanium nanoparticles.

b- Maximum tensile stress increases with both the % of titanium nanoparticles and the number of perlon layers but in an inversely proportional fashion. The ultimate tensile stress is more sensitive to the percentage of titanium nanoparticles than the number of perlon layers. Together, they contribute around 0.55 percent nanoparticles of titanium, producing a maximum tensile stress of about 85 MPa.

c- Using the response surface method and analysis of variance (ANOVA), two empirical quadratic equations for the models of bending strength at peak and maximum tensile stress with a 95% confidence level were constructed.

d- At the optimal values of titanium nanoparticles percentage (0.75%) and no. of perlon layers (10), the maximum desirable values of the mechanical properties are 94.151 MPa for peak bending strength and 90.632 MPa for maximum tensile stress with a maximum desirability value of 1.

e- The confirmation tests showed that the experimental and anticipated results are in good agreement, with a maximum error of (0.05%) for the peak bending strength and (2.90%) for the maximum tensile stress.

2- When the ideal material (0.75% and 10 Ti nano Perlon layers) was compared to the material typically used in prosthetic and orthotic centers (10 perlon layers), the fatigue endurance limit was enhanced and improved.

3- Ankle-foot orthoses made from an ideal composite material (10 perlon and 0.75% Wt. of Ti nano) have a longer lifespan and lower cost than previously available composites.

4- The patient's two legs had fewer disparities in gait analysis metrics (step time, step length, step velocity, gait cycle duration, maximum Force, etc.) when they began wearing AFOs.

5. References

[1] H. Uustal and E. Bearga, "Prosthetics and Orthotics," in *Sara Cuccurullo, M.D. (Physical Medicine and Rehabilitation Board Review)*, New York, USA: Demos Medical Publishing, 2002, pp. 409–489.

[2] M. Natália and F. Martins, "Design of Ankle Foot Orthoses using Subject Specific Biomechanical Data and Optimization Tools," in *Instituto Superior Técnico*, 2014.

[3] M. Rahman, S. Zainuddin, M. Hosur, J. Malone, M. Salam, A. Kumar, and S. Jeelani, "Improvements in Mechanical and Thermo-Mechanical Properties of E-Glass/Epoxy Composites using Amino Functionalized MWCNTs," *Composite Structures*, vol. 94, no. 8, pp. 2397–2406, 2012.

[4] B. Bedaiwi and J. Chiad, "Vibration Analysis and Measurement in the Below Knee Prosthetic Limb Part I: Experimental Work," in *ASME 2012 International Mechanical Engineering Congress and Exposition, Proceedings (IMECE)*, 2012.

[5] J. Chiad, "Study the Impact Behavior of the Prosthetic Lower Limb Lamination Materials due to Low Velocity Impactor," in *ASME 2014 12th Biennial Conference on Engineering Systems Design and Analysis (ESDA)*, 2014, pp. 25–27.

[6] M. Al-Shammari, E. Hussein, and A. Oleiwi, "Material Characterization and Stress Analysis of a Through Knee Prosthesis Socket," *International Journal of Mechanical & Mechatronics Engineering (IJMME-IJENS)*, vol. 17, no. 6, 2017.

[7] M. S. Al-Din Tahir and J. S. Chiad, "A Suggested New Material to Manufacture Above-Knee Prosthetic Socket Using the Lamination of Monofilament, Cotton, and Perlon," *Al-Nahrain Journal for Engineering Sciences (NJES)*, vol. 20, no. 4, pp. 832–837, 2017.

[8] S. Abbas, K. Resan, A. Muhammad, and M. Al-Waily, "Mechanical and Fatigue Behaviors of Prosthetic for Partial Foot Amputation with Various Composite Materials Types Effect," *International Journal of Mechanical Engineering and Technology (IJMET)*, vol. 9, no. 9, pp. 383–394, 2018.

[9] J. S. Chiad and M. S. al-Din Tahir, "A Suggested New Material to Manufacture Above-Knee Prosthetic Socket Using the Lamination of Monofilament, Cotton, and Perlon Fibers," *International Journal of Energy & Environment*, vol. 8, no. 4, 2017.

[10] M. Jweeg, Z. Hammoudi, and B. Alwan, "Optimized Analysis, Design, and Fabrication of TransTibial Prosthetic Sockets," in *IOP Conference Series: Materials Science and Engineering, 2nd International Conference on Engineering Sciences*, vol. 433, 2018.

[11] A. Abdulameer and M. Al-Shammari, "Fatigue Analysis of Syme's Prosthesis," *International Review of Mechanical Engineering*, vol. 12, no. 3, 2018.

[12] N. Yaseen, J. Chiad, and F. Abdul Ghani, "The Study and Analysis of Stress Distribution Subjected on the Replacement Knee Joint Components using Photo-Elasticity and Numerical Methods," *International Journal of Mechanical and Production Engineering Research and Development (IJMPERD)*, vol. 8, no. 6, pp. 449–464, 2018.

[13] A. Takhakh and S. Abbas, "Manufacturing and Analysis of Carbon Fiber Knee Ankle Foot Orthosis," *International Journal of Engineering & Technology*, vol. 7, no. 4, pp. 2236–2240, 2018.

[14] A. Takhakh, S. Abbas, and A. Ahmed, "A Study of the Mechanical Properties and Gait Cycle Parameter for a Below-Knee Prosthetic Socket," in *IOP Conference Series: Materials Science and Engineering, 2nd International Conference on Engineering Sciences*, vol. 433, 2018.

[15] F. Kadhim, J. Chiad, and A. Takhakh, "Design and Manufacturing Knee Joint for Smart Transfemoral Prosthetic," in *IOP Conference Series: Materials Science and Engineering, International Conference on Materials Engineering and Science*, vol. 454, 2018.

[16] L. Yousif, K. Resan, and R. Fenjan, "Temperature Effect on Mechanical Characteristics of A New Design Prosthetic Foot," *International Journal of Mechanical Engineering and Technology (IJMET)*, vol. 9, no. 13, pp. 1431–1447, 2018.

[17] J. Oleiwi and A. Hadi, "Experimental and Numerical Investigation of Lower Limb Prosthetic Foot Made from Composite Polymer Blends," *International Journal of Mechanical and Production Engineering Research and Development*, vol. 8, no. 2, pp. 1319–1330, 2018.

[18] M. Jweeg, A. Ahumdany, and A. Mohammed Jawad, "Dynamic Stresses and Deformations Investigation of the Below Knee Prosthesis using CT-Scan Modeling," *International Journal of Mechanical & Mechatronics Engineering (IJMME-IJENS)*, vol. 19, no. 1, 2019.

[19] F. Kadhim, A. Takhakh, and A. Abdullah, "Mechanical Properties of Polymer with Different Reinforcement Material Composite That used for Fabricates Prosthetic Socket," *Journal of Mechanical Engineering Research and Developments*, vol. 42, no. 4, pp. 118–123, 2019.

[20] E. Abbas, M. Jweeg, and M. Al-Waily, "Fatigue Characterization of Laminated Composites used in Prosthetic Sockets Manufacturing," *Journal of Mechanical Engineering Research and Developments*, vol. 43, no. 5, pp. 384–399, 2020.

[21] F. Kadhim, J. Chiad, and M. Enad, "Evaluation and Analysis of Different Types of Prosthetic Knee Joint Used by above Knee Amputee," *Defect and Diffusion Forum Journal*, vol. 398, 2020, pp. 34–40.

[22] F. Kadhim, A. Takhakh, and J. Chiad, "Modeling and Evaluation of Smart Economic Transfemoral Prosthetic," *Defect and Diffusion Forum Journal*, vol. 398, 2020, pp. 48–53.

[23] A. Mohammed, E. Al-Hassani, and J. Oleiwi, "The Nanomechanical Characterization and Tensile Test of Polymer Nanocomposites for Bioimplants," in *AIP Conference Proceedings*, 2019.

[24] M. Al-Shammari, Q. Bader, M. Al-Waily, and A. Hasson, "Fatigue Behavior of Steel Beam Coated with Nanoparticles under High Temperature," *Journal of Mechanical Engineering Research and Developments*, vol. 43, no. 4, pp. 287–298, 2020.

[25] M. Al-Waily, M. Al-Shammari, and M. Jweeg, "An Analytical Investigation of Thermal Buckling Behavior of Composite Plates Reinforced by Carbon Nano Particles," *Engineering Journal*, vol. 24, no. 3, 2020.

[26] E. Ahmed, A. I. Rabea, and N. Tasnim, "Nanoparticles incorporation into polymeric materials for potential improvement in the mechanical properties: A review," *Journal of Polymer Research*, vol. 27, no. 1, 2020.

[27] M. Rajan, H. El-Hamshary, and A. Al-Dhamin, "Mechanical and Tribological Properties of UHMWPE Hybrid Composites Reinforced with Halloysite Nanotubes and Graphene Oxide," *Polymers*, vol. 13, no. 3, 2021, p. 414.

[28] B. D. Khandagale and U. V. Pise, "Numerical and experimental investigation of hinged Ankle-Foot-Orthoses (AFO) using composite laminate material for Cerebral Palsy patient," *Materials Today: Proceedings*, vol. 62, pp. 2070–2080, 2022.

[29] G. Rogati et al., "A novel apparatus to assess the mechanical properties of Ankle-Foot Orthoses: Stiffness analysis of the Codivilla spring," *Journal of Biomechanics*, vol. 142, p. 111239, 2022

[30] F. S. Shahar, M. T. H. Ameed Sultan, S. N. A. Safri, M. Jawaid, A. R. Abu Talib, A. A. Basri, and A. U. Md Shah, "Physical, thermal and tensile behaviour of 3D printed kenaf/PLA to suggest its usability for ankle–foot orthosis–a preliminary study," *Rapid Prototyping Journal*, vol. 28, no. 8, pp. 1573–1588, 2022.

[31] M. J. Jweeg, H. Hamzah, M. Al-Waily, and M. A. Al-Shammari, "A Finite Element Simulation of Nano Effects on Stress Distribution in a Below Knee Prosthetic," in *IOP Conference Series: Materials Science and Engineering*, vol. 1067, no. 1, IOP Publishing, 2021, p. 012141.

[32] M. Zakaulla and S. Kesarmadu Siddalingappa, "Prediction of mechanical properties for polyetheretherketone composite reinforced with graphene and titanium powder using artificial neural network," *Materials Today: Proceedings*, vol. 49, pp. 1268–1274, 2022.

[33] F. T. Al-Maliky, J. S. Chiad, "Study and analysis the flexion moment in active and passive knee prosthesis using back propagation neural network predictive," *Journal of the Brazilian Society of Mechanical Sciences and Engineering*, vol. 44, no. 11, 2022.

[34] M. S. A.-D. Tahir, S. S. Hassan, and J. S. Chiad, "Kinematic analysis for passive multi-axes ankle joint," *Pollack Periodica*, vol. 17, no. 2, pp. 36–41, 2022.

[35] H. C. Nanotubes, "Nanomaterials Safety Considerations," 2015.

[36] M. Al-Waily, A. Deli, A. Al-Mawash, and Z. Ali, "Effect of Natural Sisal Fiber Reinforcement on the Composite Plate Buckling Behavior," *International Journal of Mechanical & Mechatronics Engineering (IJMME-IJENS)*, vol. 17, no. 1, 2017.

[37] A. H. Jeryo, J. S. Chiad, and W. S. Abbod, "Boosting mechanical properties of Orthoses - foot ankle by adding carbon Nanotube particles," *Materials Science Forum*, vol. 1039 MSF, pp. 518–536, 2021.

[38] J. Chiad, "Design, Analysis and Optimization of the Knee-Ankle-Foot Orthosis," *Gulf University Journal for Engineering and Computer Engineering*, vol. 4, no. 1, 2012.

[39] J. Chiad, M. Al-Waily, and M. Al-Shammari, "Buckling Investigation of Isotropic Composite Plate Reinforced by Different Types of Powders," *International Journal of Mechanical Engineering and Technology (IJMET)*, vol. 9, no. 9, pp. 305–317, 2018.

[40] American Society for Testing and Materials information, "Handing series 2000."